Research Square

Preprints are preliminary reports that have not undergone peer review.
They should not be considered conclusive, used to inform clinical practice,
or referenced by the media as validated information.

Differential pollen sterility in rice under high temperature stress at booting stage: ultrastructural and cytological evidence of cultivar-specific anther degradation and yield penalties

Qiuqian Hu
Yangzhou University
Guohui Li
Yangzhou University
Yi Yao
Yangzhou Polytechnic University
Jun Zhang
Yangzhou Polytechnic University
Ke Xu
Yangzhou University
Zhongyang Huo
huozy69@163.com
Yangzhou University

Research Article

Keywords: Rice, pollen abortion, tapetum, anther structure, scanning electron microscopy, transmission electron microscopy

Posted Date: July 6th, 2026

DOI: https://doi.org/10.21203/rs.3.rs-10135885/v1

License: This work is licensed under a Creative Commons Attribution 4.0 International License.
Read Full License

Additional Declarations: No competing interests reported.

Differential pollen sterility in rice under high temperature stress at booting stage: ultrastructural and cytological evidence of cultivar-specific anther degradation and yield penalties

Qiuqian Hu [1,2], Guohui Li [1,3], Yi Yao [2], Jun Zhang [2], Ke Xu [1], Zhongyang Huo [1*]

[1] Jiangsu Key Laboratory of Crop Genetics and Physiology/Jiangsu Key Laboratory of Crop Cultivation and Physiology, Agricultural College, Yangzhou University, Yangzhou 225009, China

[2] School of Landscape and Horticulture, Yangzhou Polytechnic University, Yangzhou 225009, China

[3] Jiangsu Co-Innovation Center for Modern Production Technology of Grain Crops, Yangzhou University, Yangzhou 225009, China

[*] Corresponding author, email: huozy69@163.com

Abstract

High temperature often leads to low seed setting rates and yield losses in rice, which are mainly associated with pollen abortion. However, systematic studies on the anther structure and ultrastructure changes of pollen abortion in popular cultivars are still lacking. In this pot experiment, four popular indica rice varieties (YD6, HHZ, LY6326, TYHZ) were subjected to high temperature (38°C) for 15 consecutive days from the fourth stage of panicle initiation. Using paraffin sectioning, scanning electron microscopy (SEM), and transmission electron microscopy (TEM), we systematically investigated anther wall structure, tapetum development, pollen morphology, and pollen viability, seed setting percentage and grain yield. The results revealed cultivar-specific anther damage fingerprints in four rice varieties under high temperature, characterized by distinct developmental arrest windows (pre-vacuolation arrest in LY6326, stage-10 arrest in YD6, delayed pollen starch filling in HHZ), and a comprehensive ultrastructural damage syndrome including disordered tapetum degradation, collapsed microspores with degraded protoplasm, missing exine layers (columella and tectum), and abnormal Ubisch bodies. Among the varieties, TYHZ exhibits relatively milder damage and retains some fertile pollen, indicating better heat tolerance. Furthermore, the integrated application of paraffin sectioning, SEM, and TEM establishes a multi-scale technical system for rapid and reliable screening of heat-tolerant rice germplasm.

By integrating paraffin sectioning, SEM, and TEM techniques, this study reveals the cytological features underlying yield loss and pollen abortion at the cellular morphology, surface structure, and subcellular levels in popular rice varieties exposed to high temperature

during the booting stage, offering a theoretical basis for breeding heat-tolerant rice.

Keywords: Rice; pollen abortion; tapetum; anther structure; scanning electron microscopy, transmission electron microscopy

1. Introduction

In recent years, several extreme heat events have occurred during the rice growing season, especially in the main rice producing areas in the middle and lower reaches of the Yangtze River, posing serious challenges to rice safety production.

Global warming has significantly increased the frequency of high temperatures, posing a serious threat to crop production and global food security(Zandalinas et al. 2021; Xiao et al. 2025). As one of the main food crops, rice also faces many challenges in terms of safe production(Peng et al. 2004; Visakh et al. 2024; Khan et al. 2026; Xu et al. 2021; Sun et al. 2025). Research has shown that high temperatures can lead to a decrease of about 40% in rice yield (Xiong et al. 2017), when the daytime temperature exceeds the optimum, each 1 °C increase leads to a 7% reduction in rice yield(Su et al. 2023). In recent years, the intensity and duration of high temperatures have shown an increasing trend. In the summer of 2022, the rice growing areas in the middle and lower reaches of the Yangtze River experienced a record high intensity and duration of high temperatures, with more than 20 days of high temperatures above 35℃. Multiple meteorological stations recorded data showing that the number of high temperature days broke the maximum number of high temperature days observed since 1951(Hao et al. 2022). However, from mid to late July to September, which is the booting stage or flowering period of most rice varieties, prolonged high temperatures of 35℃ for more than 3 days can affect the flowering and fruiting of rice, reducing rice yield (Das et al. 2014). Under future climate scenarios, the number of extreme heat daysin southern China is expected to rise by 12–18 days by the 2080s relative to 1981–2014, which is the highest increase compared with other regions or scenarios, which will seriously threaten the safe production of rice in the middle and lower reaches of the Yangtze River (Chen et al. 2025). High temperature damage to rice mainly occurs reproductive growth

stage, the frequency of high temperature occurrence from the booting stage to the heading stage is much higher than other growth stages of rice(Jiang et al. 2024).

The pollen formation are crucial throughout the entire lifecycle of flowering plants(Hu et al. 2021). The booting stage is a critical period for anther and pollen development, which is closely related to pollen viability and final yield formation (Hu et al. 2021; Hu et al. 2024; Yamamori et al. 2021). Our previous research found that the high temperature during the panicle initiation stage leads to abnormal anther development, which is an important reason for rice pollen sterility, spikelet sterility and yield loss. However, the anther structural changes are limited to one two-line hybrid rice variety, which is no longer grown in production, the small sample size resulted in weak persuasiveness. Previous studies found that high-temperature resistance of Qianjiang 3, Huanghuazhan and N22 during the young panicle differentiation stage is unstable, and different experimental results of high-temperature resistance are obtained for the same variety at the same temperature (Hu et al. 2025; Chen et al. 2026; Chen et al. 2023). At different stages of young panicle development, the seed setting percentage varies greatly under the same high-temperature treatment. High-temperature treatment from the stamen and pistil formation stage to the meiosis stage has the greatest negative impact on the seed setting rate, even resulting in total reproduction failure(Hu et al. 2025; Chen et al. 2026); however, there are still few studies on these varieties in-depth microscopic and ultrastructural characteristics of anther.

In this study, we investigated the **anther structure and ultrastructure changes of four popular varieties induced by high temperature stress** during the booting stage (the fourth stage of panicle initiation to pre-anthesis). The four indica rice varieties used in this study—YD6 (Yangdao 6), HHZ(Huanghuazhan), LY6326 (Liangyou 6326), and TYHZ (Tianyou Huazhan), which represent different genetic backgrounds and cultivation profiles in the middle and lower reaches of the Yangtze River. YD6 is a classic conventional indica variety that was bred by the Lixiahe Area Agricultural Research Institute of Jiangsu Province and has served as an excellent male parent for many hybrid rice combinations(Xu et al. 2001), with a cumulative planting area of over 7 million hectares (including its derivatives). HHZ is another widely cultivated

conventional indica variety known for its stable yield and good grain quality, which was bred by the Rice Research Institute of Guangdong Academy of Agricultural Sciences using the core germplasm breeding theory(Zhou et al. 2012), its heat tolerance at the flowering stage has been reported in previous studies (Guo et al. 2024; Wu et al. 2019). LY6326 is a two-line hybrid indica combination that has been extensively planted(Wang et al. 2007), with a cumulative area exceeding 450,000 hectares, TYHZ is a three-line hybrid indica combination with a cumulative area exceeding 600,000 hectares. Their high temperature sensitivity will provide a reliable baseline for comparing the responses of hybrid varieties and underscores the need for high temperature-tolerant alternatives in regions prone to high-temperature events. The result will provide foundation for reducing the yield loss of rice in the middle and lower reaches of the Yangtze River and selecting high-temperature resistant varieties.

2. Materials and methods

2.1 Plant material and growth conditions

A pot experiment was performed during the rice growth season from May to October 2022 at the experimental station of Yangzhou University, Yangzhou, Jiangsu Province, China (32◦24′ N, 119◦26′ E). Four rice genotypes YD6, HHZ, LY6326, TYHZ were used. YD6 and HHZ are conventional indica rice, the growth period of YD6 and HHZ is 145 and 120, respectively; while LY6326 and TYHZ are hybrid indica rice, LY6326 is indica two-line super hybrid rice, growth period is 141, while TYHZ is indica three-line super hybrid rice, growth period is 123 days.

Rice seeds were sunbathing on a sunny day and then put in oven for 2 days at 50 °C for breaking dormancy, sown in perforated plastic seeding trays with seedling substrate on 24 May. After 20 days, rice seedlings of uniform size were transplanted into a 15 L plastic pot (30 cm height × 25 cm top diameter) on 15 June, Transplanted one seedling per hole, with three seedlings per pot. The pots were filled with 15 kg air-dried, which was a sandy loam that prepared from the local paddy field. Phosphate

fertilizer (2.25 g P pot^{-1}) in the form of calcium super-phosphate, while potassium fertilizer (2.25 g K pot^{-1}) in the form of potassium chloride was applied as basal fertilizer. The nitrogen fertilizer is calculated according to the fertilizer amount of 200 kg/ha in the field. A total of 3.60 g N pot^{-1} was applied as urea with three splits: 1.44 g N pot^{-1} as basal fertilizer, 0.72 g N pot^{-1} top-dressed 12 days after transplanting, and 1.44 g N pot^{-1} applied as panicle fertilizer. The potted plants were placed outdoors in three replicates, 10 pots for each variety and each temperature treatment per one replicate. All plants were artificially watered with tap water each day, and the surface water layer in the pots was kept in approximately 2 cm during the entire growth season. Additionally, fine management was performed during the whole growth season.

High temperature treatments were performed using two individual greenhouses (4.1 m in length, 3.0 m in width, and 2.2 m in height), the greenhouses were purchased from Beijing Yishengtaihe company. The temperature treatments were performed after the end of third stage of young spikelet differentiation. Panicle initiation stage were divided into 7 stages according to Hu et al. (2021). In this study, high temperature treatment was imposed for 15 consecutive days from the fourth stage of panicle initiation. For the high temperature (HT) treatment, the daytime temperatures were set at 38°C from 07.00–19.00 h, whereas the daytime temperature was 30°C for the control temperature (CK) treatment. The nighttime temperature for both temperature treatments was set at 26°C from 19.00–07.00 h. The daytime relative humidity was set at 70% for both treatments. The HOBO sensors (MX2301A, Onset Computer Corporation, Bourne, MA, USA) were installed at the rice canopy, temperature and relative humidity were record every 30 min. The data was exported from mobile phone HOBO mobile software. The actual daytime average maximum temperature under HT was 38.1°C, which was 8.0°C higher than that of the CK treatment. The actual mean daytime temperature during the whole HT duration was 34.7°C, which was 6.6°C higher than that of the CK treatment. The mean daytime relative humidity of the CK treatment was 65.5% and 78.3% for the HT treatment. The mean daytime relative humidity of the CK treatment was 65.5% and 78.3% for the HT treatment. The mean nighttime temperature were 26.6°C and 24.6 °C for CK and HT treatment, respectively. The mean nighttime relative

humidity was 89.0% and 89.5% for CK and HT treatment, respectively.

2.2 Determination of yield and seed setting percentage

At maturity, the rice yield and seed setting rate were sampled and calculated. Shortly, three plants were harvested from three separated pots and divided into different parts of leaves, stems and panicles. All grains on the panicle are manually threshed and divided into two groups, including full grain and non-filled grain, which were counted and seed setting rate were calculated. The filled grains were measured after oven drying at 80℃ to a constant weight. Then, the yield was determined according to 14% moisture content.

2.3 Observation of anther structures using paraffin section

Anthers in spikelets at stage 10 and stage 13 were collected. After fixing in FAA for 24 hours, the anthers undergo a series of steps including paraffin embedding, dewaxing, staining, and sealing, and finally transverse sections were observed under an optical microscope.

Specifically, firstly, the anthers in FAA solution were taken and dehydrated in a gradient of ethanol solutions: 5 min each in 70% ethanol and 10 min each in 85%, 95% and 100%. Secondly, the anthers were placed into 1/2 xylene (50%) for 20 min, xylene (100%) for 20min, repeat once for clearing. Thirdly, paraffin infiltration and embedding. Fourthly， sectioning, the middle part of the anther were cut using microtome(RM2016, Leica technology company, Shanghai). Fifthly, transverse sections were placed into 1/2 xylene (50%) for 20 min, xylene (100%) for 20min, repeat once, sequentially, 30%, 50%, 75% alcohol for 5min, wash with tap water, and dewax. Sixthly, slices were stained in toluidine blue dye solution for 1-2 hours, then rinse with tap water to remove excess dye. Seventhly, immerse them in a gradient of 50%, 70%, and 80% alcohol for 5 seconds each, followed by dehydration in three tanks of anhydrous ethanol and put them into clean xylene for 5 minutes, seal with neutral gum. Finally, transverse sections of anthers were performed optical microscopy (Nikon Eclipse E100) and image

acquisition analysis.

2.4 Observation of anther structures using scanning electron microscope

The observation of the ultrastructure of anthers under scanning electron microscopy requires a series of steps such as fixation, dehydration, drying, mounting, and gold spraying before they can be observed. Specifically, approximately 60 mature fresh anthers at stage 13 were harvested and immediately submerged in 2 mL of 2.5% glutaraldehyde (v/v) in 0.1 M sodium phosphate buffer (pH 7.2), overnight at 4℃. After washing the sample 3-4 times in 0.1 M phosphate-buffered saline (PBS), the anthers wrapped in soft tissue paper were then dehydrated in a gradient of ethanol solutions: 15 min each in 30%, 50%, and 70% ethanol and 10 min each in 80%, 90%, 95% and 100% (add anhydrous sodium sulfate, Na_2SO_4). The fixed samples were dried with liquid CO_2 using a critical point dryer (CPD-300) and then mounted with the side to be observed facing upward onto the sample stage. Make the sample conductive by sputter-coating the surface with gold in an ion sputter (SCD-500). Afterwards, and the characteristics of anther wall and pollen grain were observed using a scanning electron microscope (GeminiSEM 300 FESEM, Carl zeiss microscopy Gmbh, Oberkochen, Germany).

2.5 Observation of anther structures using transmission electron microscopy.

Fresh anthers at stage 10 were pre-fixed in 2.5% glutaraldehyde in phosphate buffer (pH 7.4) for 4 h. The samples were then post-fixed in 1.0% OsO_4 at room temperature in the same phosphate buffer for 2 h. Then, they were dehydrated in ascending graded series of alcohol (50%, 70%, 80%, 90%, 95%, 100%, 100% alcohol for 15 minutes each time) and was infiltrated overnight in a mixture (acetone: embedding agent is 1:1), while pure embedding agent was infiltrated overnight. Sections of 1 mm thick were made on a microtome (Leica UC7, Leica). Ultrathin sections of 60—80 nm were made using an ultramicrotome (DiatomeUltra 45°, Nidau, Canton Bern, Switzerland), to observe the effects of high temperature on the ultrastructure of anther with TEM. The sections were examined using transmission

electron microscopy (Tecnai G2 20 TWIN, FEI). The photomicrographs obtained were used to assess the ultrastructure of the anther walls and pollen grains.

3. Statistics

The value for a given trait was expressed as the mean of three replicates with standard error (SE) using the Excel. Differences between the two temperature treatments for the four cultivars were evaluated at a 5% probability level using the least significant difference (LSD) test of Statistix 9 software package (Analytical software, Tallahassee, FL, USA). The value for pollen viability was expressed as the mean of three replicates with standard error (SE) using the SigmaPlot 10.0 software package (SPSS Inc., Chicago, IL, USA).

4. Results

An average temperature of 35.6°C in the greenhouse under daytime high-temperature treatment, which was 6.8°C higher than the control. The average daytime humidity was 66.4%, representing an increase of 3.6 percentage points compared to the control. The maximum daytime temperature reached 37.3°C, exceeding the control by 5.5°C. The nighttime temperature was 24.9°C, which was 0.5°C lower than the control, while the nighttime humidity levels were 73.0% and 66.1%, respectively (Table 1).

Table 1

Ambient temperature and relative humidity in controlled chamber at booting stage

T	Mean daytime T	Mean daytime relative humidity	Daytime maximum T	Mean nighttime T	Mean nighttime relative humidity
	℃	%	℃	℃	%
CK	28.1	65.5	30.1	26.6	89.0
HT	34.7	78.3	38.1	24.6	89.5

Table 2

High temperatures lead to a significant reduction in the yield of all four varieties. Compared to the control group, high temperatures caused the seed-setting rates of YD6, HHZ, LY6326, and TYHZ to decrease by 92.0%, 77.8%, 95.9%, and 45.2%, respectively. Correspondingly, high temperatures resulted in yield reductions of 94.7%, 80.6%, 97.6%, and 53.1% for YD6, HHZ, LY6326, and TYHZ, respectively. The decline in seed-setting rate was the primary factor contributing to the yield reduction.

Table 2 Yield and seed setting percentage of four rice cultivars under high temperature at booting stage

Variety	T	Seed setting percentage (%)	Yield (g plant^{-1})
YD6	CK	73.8±5.4 B a	41.1±3.7 B a
	HT	5.9±1.5 C b	2.2±0.3 BC b
HHZ	CK	57.5±7.8 C a	20.4±0.2 C a
	HT	12.8±5.7 B b	4.0±1.7 B b
LY6326	CK	88.6±1.8 A a	52.6±4.5 A a
	HT	3.6±1.4 C b	1.3±0.6 C b
TYHZ	CK	67.6±5.9 B Ca	45.6±6.5 AB a
	HT	37.0±1.0 A b	21.4±0.6 A b

Notes: CK control temperature, HT high temperature. Data are the average of three replicates ± standard deviation (n = 3). The different upper-case letters indicate significance between the cultivar treatments for the same temperature using the least significant difference (LSD) at $P < 0.05$. The different lower-case letters indicate significance between the temperature treatments for the same cultivar using the least significant difference (LSD) test at at $P < 0.05$.

The plump, red, circular pollen grains represent fertile pollen, while the pale, non-plump, and non-circular pollen grains indicate abortive pollen (Fig.1 A-H). Statistical analysis revealed that high temperatures significantly reduced pollen fertility across all four varieties, although the extent of reduction varied significantly among them (Fig. 1 I). Compared to the control group, high temperatures caused reductions in pollen fertility of 19.1% in YD6, 16.3% in HHZ, 56.8% in LY6326, and 14.5% in TYHZ, respectively (Fig. 1 I).

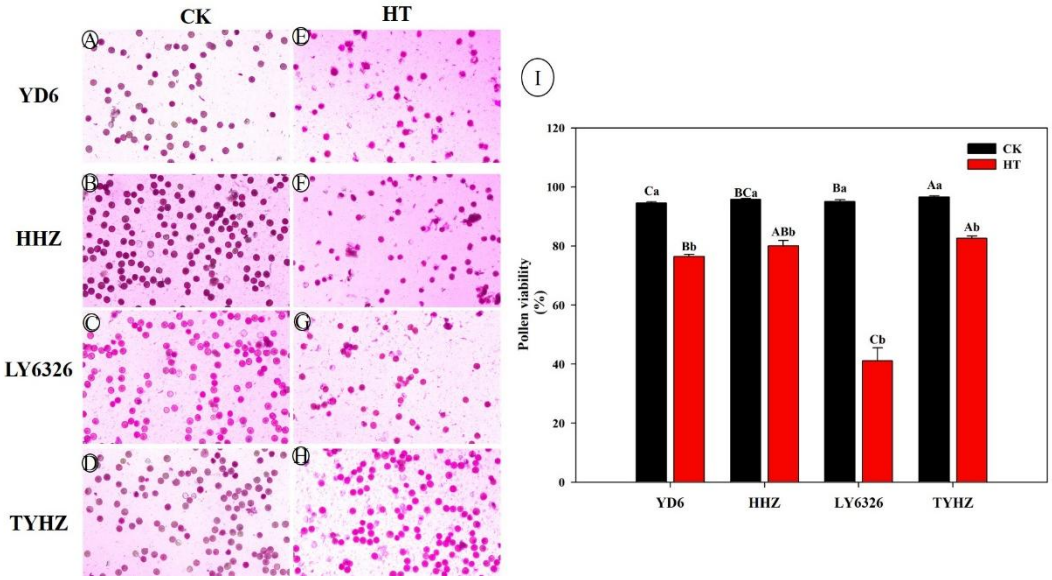


Fig. 1 Pollen viability of four rice cultivars under high temperature at booting stage

Notes: CK control temperature, HT high temperature. Data are the average of three replicates ± standard deviation (n = 3). For each replicate, five fields of view were captured to assess pollen fertility. The different upper-case letters indicate significance between the cultivar treatments for the same temperature using the least significant difference (LSD) at $P < 0.05$. The different lower-case letters indicate significance between the temperature treatments for the same cultivar using the least significant difference (LSD) at $P < 0.05$.

Fig. 2

Paraffin sections of anthers at two stages were stained with toluidine blue. Under control temperature, at anther development stage 10, the microspores were vacuolated, regularly round, and closely adhered to the tapetum cells in the anther wall (Fig. 2A). High temperature caused varying degrees of anther malformation in the four varieties (Fig. 2 B-J). High temperature caused one anther locule of YD6 to become narrow in space; in the other three locules, the spores failed to vacuolate normally and did not closely adhere to the anther wall, and the tapetum cells were scattered near the endothecium (Fig. 2B). High temperature caused the anther wall of HHZ to thicken, epidermal cells to enlarge, and microspores also failed to vacuolate normally, not forming regularly round vacuolated spores (Fig. 2C). High temperature caused the four anther locules of LY6326 to become narrow and elongated, with spores crowded

together and stained deeply by toluidine blue; there were no vacuolated spores in the locules that could continue developing into normal pollen (Fig. 2D). High temperature also caused the anther locules of TYHZ to become narrow and elongated, with a reduced number of spores in the locules and an increased number of irregularly shaped spores (Fig. 2E).

Under control temperature, at anther development stage 13, the four anther locules were regularly round, with many fertile pollen grains in the locules; the cells were completely filled with storage substances such as starch, the pollen grains were round, and the number of sterile pollen grains per locule was very low (Fig. 2F). High temperature caused a significant reduction in fertile pollen grains per locule in YD6; some locules even had no fertile pollen grains. The aborted spores were incompletely developed, shriveled in morphology, and arrested at anther development stage 10 (Fig. 2G). Under high temperature, the number of fertile pollen grains in HHZ decreased sharply; the few fertile pollen grains in the locules were still at the content-filling stage, showing severe developmental delay (Fig. 2H). High temperature caused a significant reduction in the number of fertile pollen grains per locule in LY6326. In some locules, spores and anther walls were disorganized; in others, aborted spores were arrested at anther development stage 10; in still others, pollen grains were still at the filling stage (Fig. 2I). Under high temperature, the four anther locules of TYHZ became narrow and elongated, and the fertile pollen grains in the locules were still at the content-filling stage, showing developmental delay (Fig. 2J).

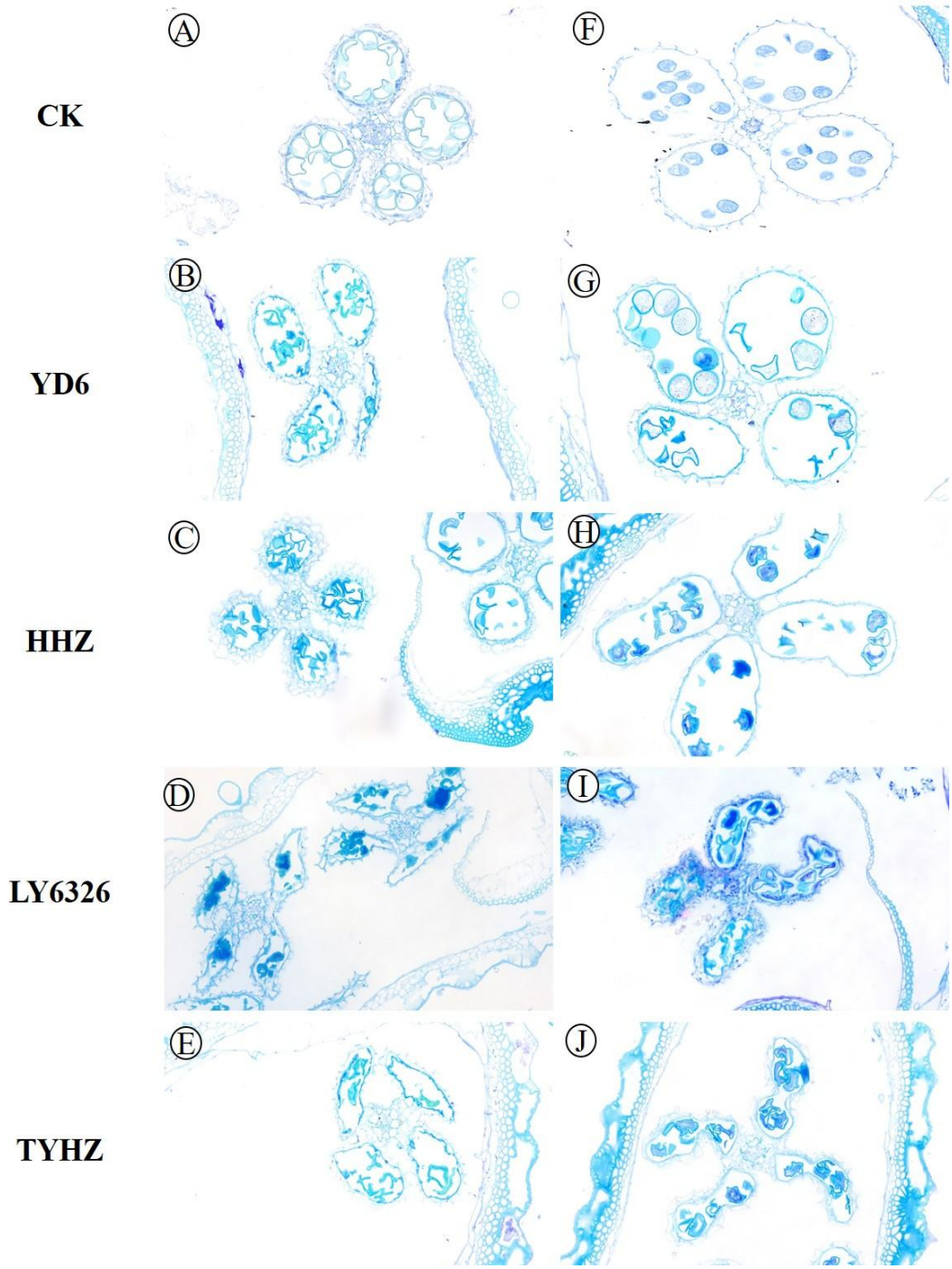


Fig. 2 Anther morphological structure at stage 10 and stage 13 of the four rice cultivars under high temperature at booting stage.

Notes: light microscopy images of transverse section of anther following 15 days exposed to either control (30℃) conditions (A, F) or high temperature stress (38℃) treatment at stage 10 (B-E) and stage 13 (G-J). Representative control cross-sections from Huanghuazhan; other three cultivars showed identical patterns (images not shown).

Fig. 3

Under scanning electron microscopy (SEM), it was clearly observed that under control temperature, the pollen grains within the four anther locules of YD6 were regularly spherical (Fig. 3F). The surface of the pollen grains was smooth (Fig. 3A). The germinal pore was located at the center of the pollen grain (Fig. 3B). Sporopollenin was uniformly deposited (Fig. 3C), and Ubisch bodies were evenly distributed (Fig. 3D). The cuticle ornamentation on the outer anther wall appeared as an interwoven meshwork (Fig. 3E). Under high temperature, although the pollen grains of YD6 were still regularly round, they were covered with some unidentified substances (Fig. 3G), and the germinal pore developed abnormally (Fig. 3 H, L). Sporopollenin deposition was uneven (Fig. 3 I). Ubisch bodies were abnormal in morphology, with indistinct punctate protrusions (Fig. 3J). The cuticle ornamentation on the outer anther wall became a dense interwoven meshwork (Fig. 3K).

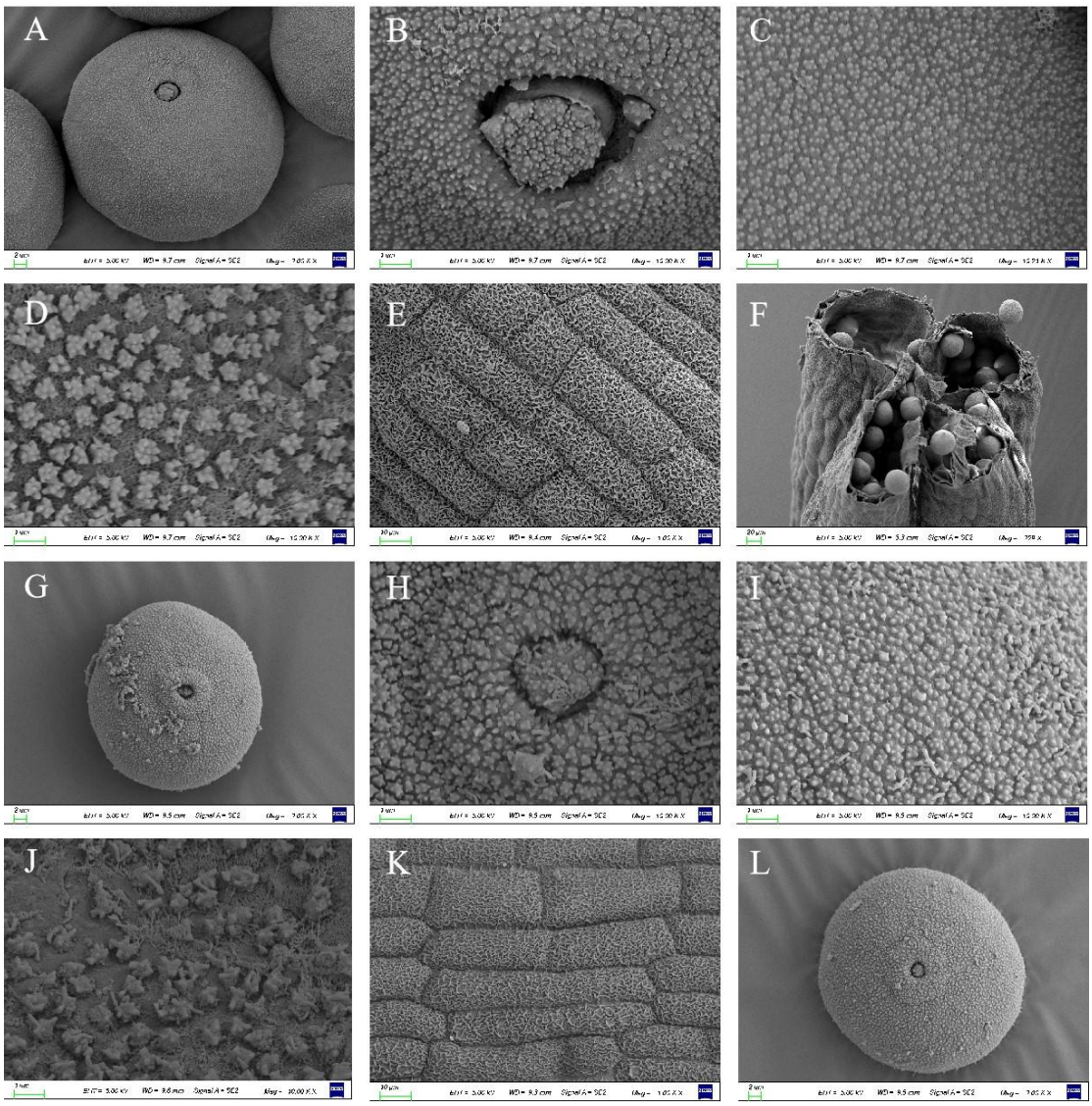


Fig. 3 Morphological changes of mature anther and pollen grains induced by high temperature stress in rice cultivars YD6.

Notes：Scanning electron microscopy images of anther following 15 days exposed to either control (30℃) conditions (A-F) or high temperature stress (38℃) treatment (G-L). A, G, L, single pollen grain, scale bars = 2 μm; B, H, Pollen germination pore, scale bars = 1 μm; C, I, pollen grain surface sculpture, scale bars = 1 μm; D, K, Ubisch body, scale bars = 1 μm; E, L, Anther epidermis, scale bars = 10 μm; F, Cross section of anther, scale bars = 20 μm.

Under control temperature, the pollen grains of HHZ were regularly round (Fig. 4A). The germinal pore was located at the center of the pollen grain (Fig. 4B). Sporopollenin was uniformly deposited (Fig. 4C), and Ubisch bodies were evenly distributed (Fig. 4D). The cuticle ornamentation on the outer anther wall appeared as an interwoven meshwork (Fig. 4E). Within the anther locule, most pollen grains were

regularly round, with a small number of shriveled pollen grains (Fig. 4F). Under high temperature, the pollen grains of HHZ were severely shriveled, and the number of shriveled pollen grains per anther locule increased (Fig. 4L). The pollen grains were covered with many unidentified substances (Fig. 4G), and the germinal pore with abnormal operculum appearing very small and not protruding, (Fig. 4G). Sporopollenin deposition showed no significant difference compared to the control (Fig. 4I). Ubisch bodies were abnormal in morphology and sparsely distributed (Fig. 4I). The cuticle on the outer anther wall lacked a dense interwoven meshwork ornamentation (Fig. 4K).

Fig. 4

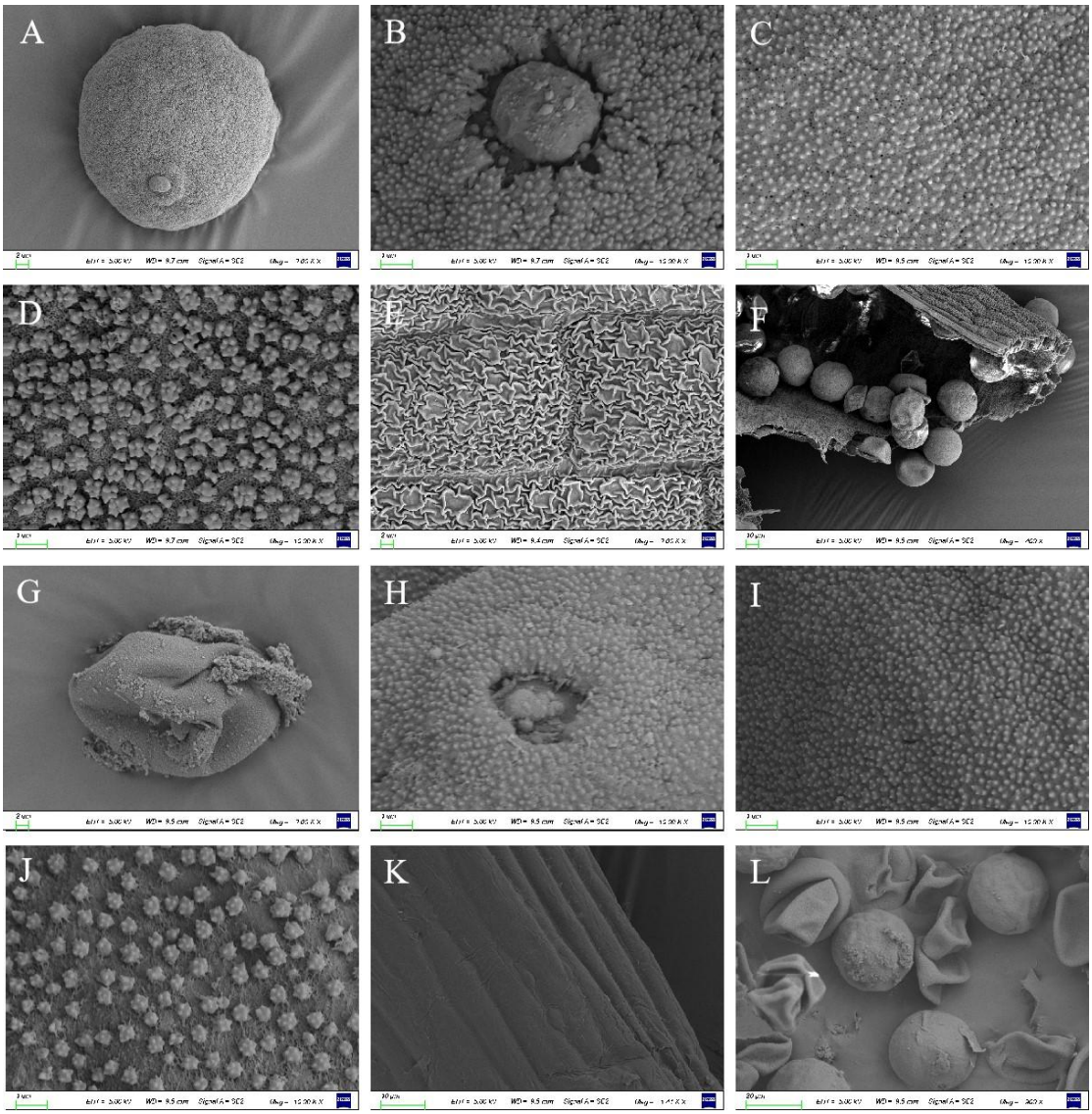


Fig. 4 Morphological changes of mature anther and pollen grains induced by high temperature stress in rice cultivars HHZ.

Notes: Scanning electron microscopy images of anther following 15 days exposed to either control (30℃) conditions (A-F) or high temperature stress (38℃) treatment (G-L). A, G, single pollen grain, scale bars = 2 μm; B, H, Pollen germination pore, scale bars = 1 μm; C, I, pollen grain surface sculpture, scale bars = 1 μm; D, J, Ubisch body, scale bars = 1 μm; E, K, Anther epidermis, scale bars = 10 μm; F, L, pollen grains; F, scale bars = 10 μm. L, scale bars = 20 μm.

Fig. 5

Under control temperature, the pollen grains of LY6326 were regularly spherical (Fig. 5A). The germinal pore was located at the center of the pollen grain (Fig. 5B). Sporopollenin was uniformly deposited (Fig. 5C), and Ubisch bodies were evenly distributed (Fig. 5D). The cuticle ornamentation on the outer anther wall appeared as an interwoven meshwork (Fig. 5E). Regularly spherical pollen grains were observed inside the anther locule (Fig. 5F). Under high temperature, the pollen grains of LY6326 were severely shriveled. In a few shriveled pollen grains, the germinal pore could not be observed (Fig. 5G). Few individual pollen grains were distributed within the anther locule (Fig. 5H). The spores were tightly and orderly arranged on the tapetum (Fig. 5H, L). No Ubisch bodies were visible on the inner anther wall, which appeared smooth (Fig. 5I, J). Sporopollenin deposition became denser compared to the control (Fig. 5G). The dense interwoven meshwork ornamentation of the cuticle on the outer anther wall was not clearly distinguishable (Fig. 5K).

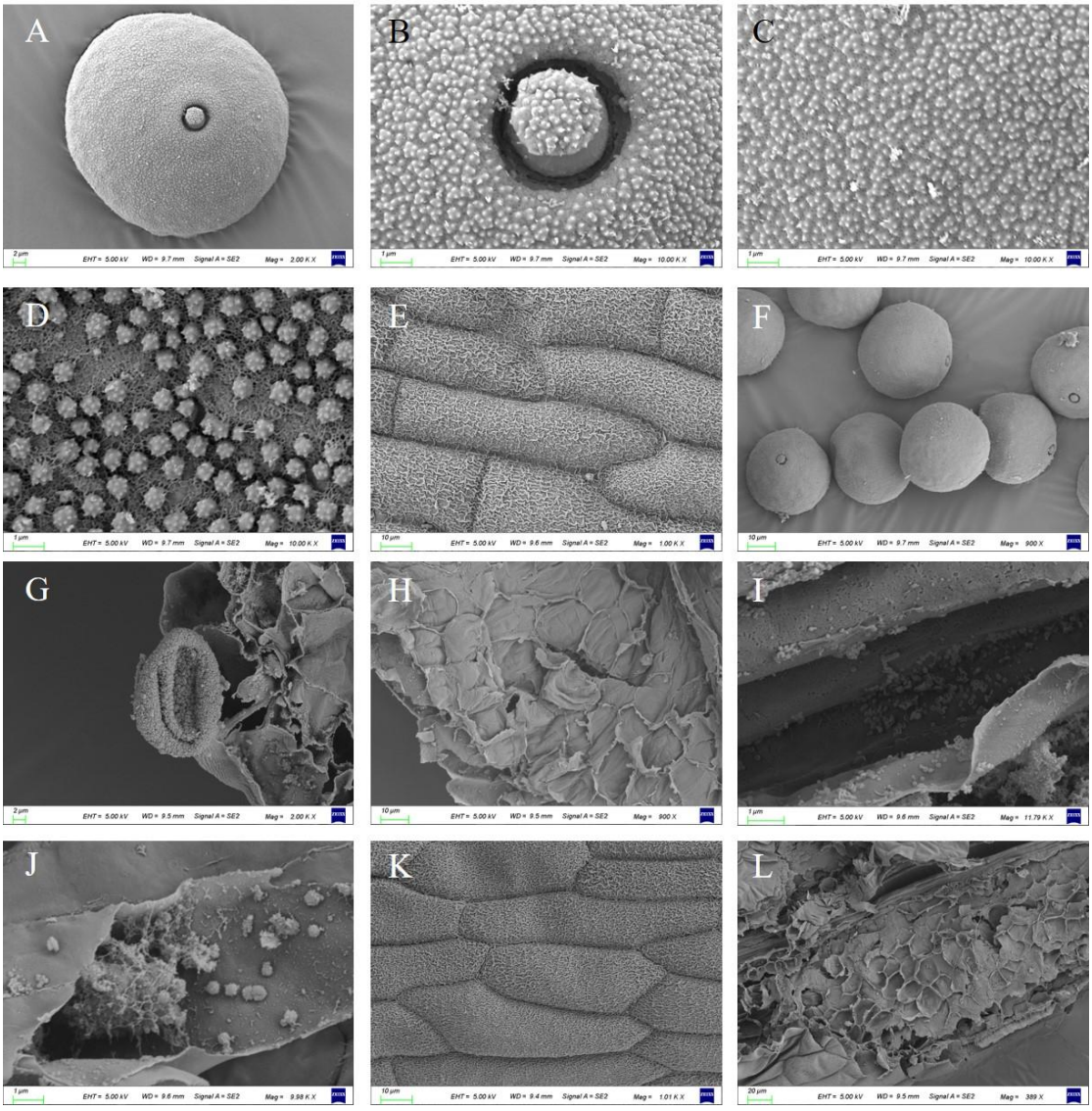


Fig. 5 Morphological changes of mature anther and pollen grains induced by high temperature stress in rice cultivars LY6326.

Notes: Scanning electron microscopy images of anther following 15 days exposed to either control (30℃) conditions (A-F) or high temperature stress (38℃) treatment (G-L). A, G, H, single pollen grain, scale bars = 2 μm; B, Pollen germination pore, scale bars = 1 μm; C, I, pollen grain surface sculpture, scale bars = 1 μm; D, J, Ubisch body, scale bars = 1 μm; E, K, Anther epidermis, scale bars = 10 μm; F, L, pollen grains; F, scale bars = 10 μm. L, scale bars = 20 μm.

Fig. 6

Under control temperature, the pollen grains of TYHZ were regularly spherical (Fig. 6A). The germinal pore was located at the center of the pollen grain (Fig. 6B). Sporopollenin was uniformly deposited (Fig. 6C), and Ubisch bodies were evenly distributed (Fig. 6D). The cuticle ornamentation on the outer anther wall appeared as an interwoven meshwork. Compared with the other three varieties, the grooves on the epidermal surface were inconspicuous (Fig. 6E). The pollen grains inside the anther locule were all regularly spherical (Fig. 6F). Under high temperature, the pollen grains of TYHZ became flattened and were not filled with contents (Fig. 6G). The germinal pore could still be observed on the shriveled pollen grains (Fig. 6H). The deposition density of sporopollenin on the pollen exine increased (Fig. 6I). The density of Ubisch bodies on the inner anther wall increased (Fig. 6J). The interwoven meshwork of the cuticle on the outer anther wall was denser than that of the control (Fig. 6K). Overall, about 60% of the pollen grains were not filled with contents such as starch, appearing flattened and shriveled (Fig. 6L).

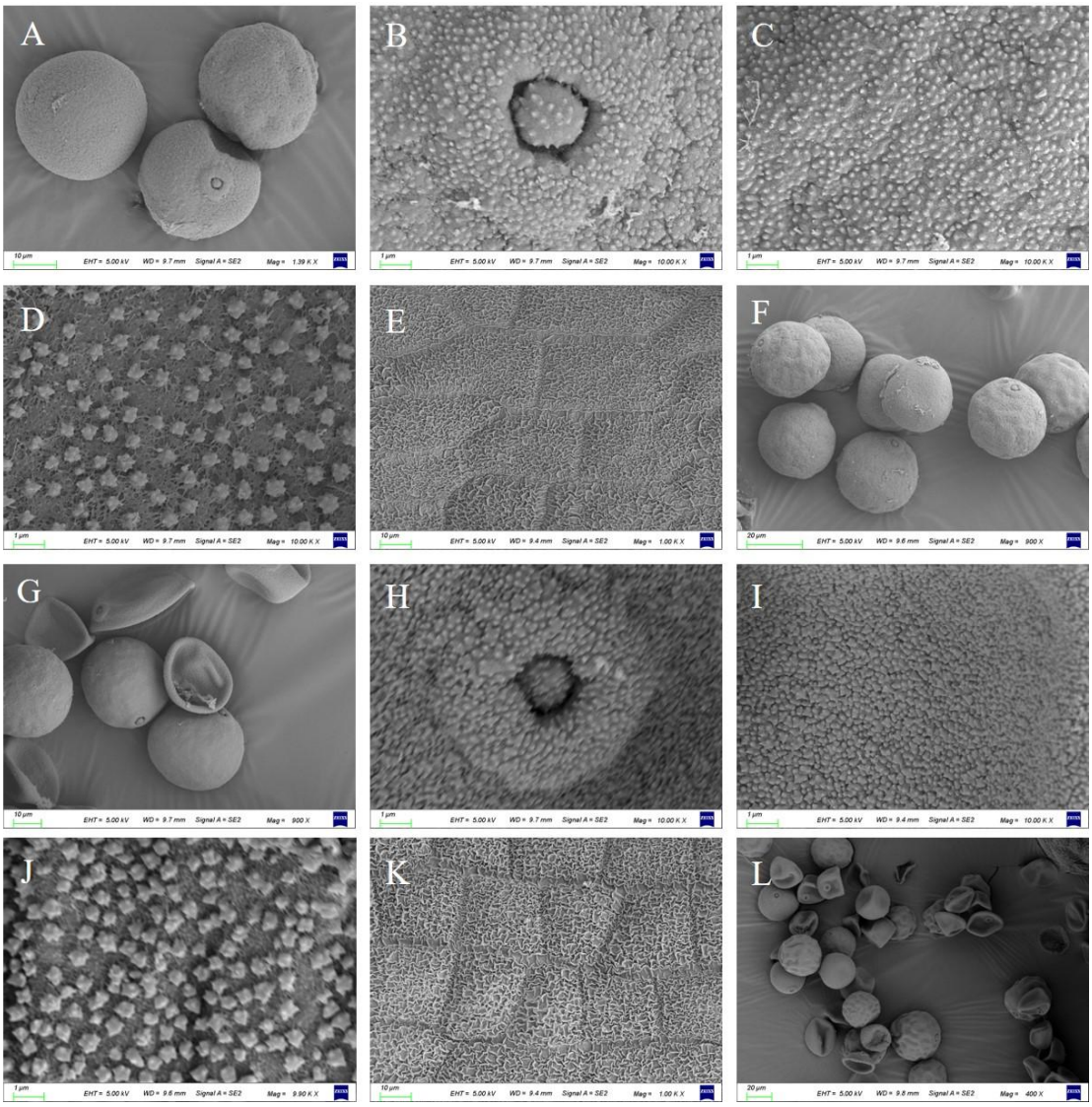


Fig. 6 Morphological changes of mature anther and pollen grains induced by high temperature stress in rice cultivars TYHZ.

Notes: Scanning electron microscopy images of anther following 15 days exposed to either control (30°C) conditions (A-F) or high temperature stress (38°C) treatment (G-L). A, G, pollen grains, scale bars = 10 μm; B, H, pollen germination pore, scale bars = 1 μm; C, I, pollen grain surface sculpture, scale bars = 1 μm; D, J, Ubisch body, scale bars = 1 μm; E, K, Anther epidermis, scale bars = 10 μm; F, L， pollen grains, scale bars = 20 μm.

Anther development at stage 10 is a period following the completion of the meiotic stage in anthers, and its phenotype reflects the post-meiotic outcome. Under control temperature, the anther wall, vacuolated microspores and pollen exine characteristics of the four varieties were essentially consistent; therefore, only the anther wall and vacuolated microspores morphology of HHZ under control temperature are presented. The middle layer degenerates, leaving three layers of the anther wall: the epidermis,

endothecium, and tapetum. The tapetum cells degenerate and contain almost no inclusions (Fig. 7A). Vacuolated spores begin to accumulate contents such as starch and lipids, and the vacuolated spores closely adhere to the anther locule wall (Fig. 7B). The exine of the vacuolated spores has a clear outline, with a clear outer exine layer, columella layer, and tectum (Fig. 7 C). Under high temperature, transmission electron microscopy revealed varying degrees of abnormal development in all four varieties (Fig. 7 E-T). The details are as follows:

For YD6, the entire anther locule is extremely irregular, shriveled into a narrow and elongated shape. The epidermal cells are not regularly elliptical but become elongated; the endothecium cells contain no inclusions; the tapetum cells lack distinct cell walls, and their contents fill the entire locule (Fig. 7E). There is almost no space between the epidermis, endothecium, tapetum, and spores, which are filled with granular inclusions (Fig. 7F). HT causes the spores of YD6 to collapse, with degradation of protoplasm and organelles; the exine outline of the vacuolated spores becomes blurred, and the columella layer is no longer visible (Fig. 7G). The Ubisch bodies distributed on the tapetum cell walls are disorganized (Fig. 7H).

HT causes secondary wall thickening in the endothecium of HHZ (Fig. 7I). The tapetum does not degenerate, and the tapetum cells become hypertrophied (Fig. 7J). The vacuolated spores collapse, with degradation of protoplasm and organelles; the exine continuity of the spores is interrupted (Fig. 7K), the exine outline is blurred, and the columella layer and tectum are absent. The distribution of Ubisch bodies is related to the morphology of the tapetum cells (Fig. 7L).

HT does not affect the epidermal cell morphology of LY6326 anthers, but the endothecium cells increase in size, lack electron-dense material, appear transparent, and the endothecium begins to thicken. The tapetum cells have distinct cell walls, but the walls become thinner (Fig. 7M, N). Unevenly distributed Ubisch bodies are present outside the cells. The vacuolated spores collapse, shrinking into a thread-like shape, with degradation of protoplasm and organelles (Fig. 7O). The spore exine shows no continuity interruption, but the exine outline is blurred, and the columella layer and tectum are absent (Fig. 7P).

HT causes almost complete degeneration of the tapetum in TYHZ, leaving only the epidermal layer, but the epidermal cells become elongated and exhibit protrusions (Fig. 7Q). Unevenly distributed Ubisch bodies are present outside the tapetum cells. The vacuolated spores collapse and shrink into irregular shapes (Fig.7R), with degradation of protoplasm and organelles (Fig.7S). Some spores show interruption of exine continuity, and the exine outline is blurred, with no columella layer or tectum (Fig. 7T).

Synthesizing the TEM results of the four varieties at anther development stage 10, it is found that abnormal spore development shape and abnormal exine morphology are common features among all four varieties. Regarding the anther wall, the tapetum of LY6326 and TYHZ degenerates prematurely, the tapetum cells of HHZ show delayed degeneration, and YD6 exhibits abnormal degeneration, with the anther locule filled with tapetal degradation contents (Fig. 7).

Fig. 7

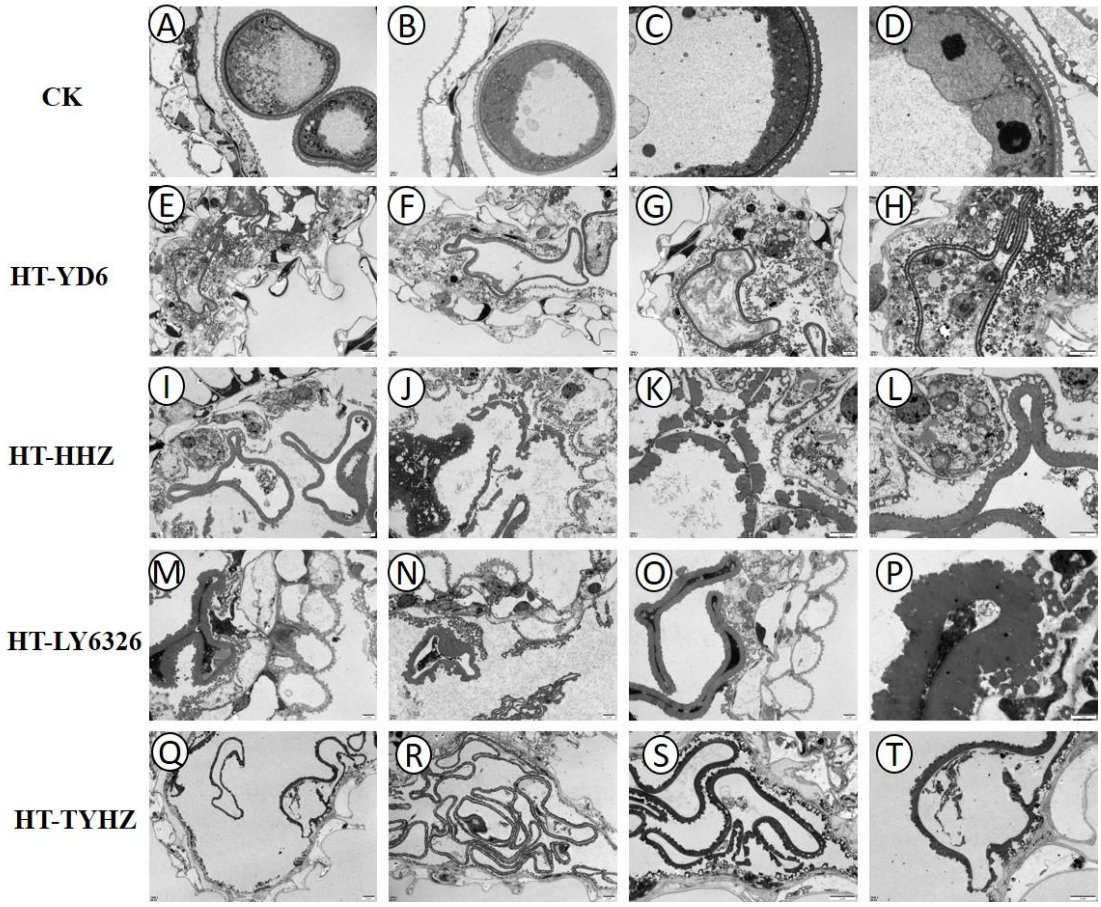


Fig.7 Anther wall and pollen morphological structure of the four rice cultivars under high temperature at booting stage.

Notes: Transmission electron microscopy images of anther cross-sections following 15 days exposed to either control (30℃) conditions (A-D) or high temperature stress (38℃) treatment (E-T). A, E, I, M, Q, anther wall; B, F, J, N, R, tapetum; C, G, K, O, S, microspore; D, H, L, P, T, pollen wall. Representative control cross-sections from Huanghuazhan; other three cultivars showed identical patterns (images not shown).

5. Discussion

5.1 Varietal differences in heat tolerance

In this study, four indica rice varieties (YD6, HHZ, LY6326, TYHZ) were subjected to high-temperature treatment at the booting stage, the results showed that YD6 and HHZ are generally considered sensitive to high temperature, the sensitivity of

YD6 and HHZ was confirmed by previous study in flowering(Guo et al. 2024; Wu et al. 2019), Whereas HHZ show inconsistent high-temperature tolerance at the panicle differentiation stage(Hu et al. 2025). Therefore, it is essential to distinguish different stages when evaluating the heat tolerance of a variety.

Despite LY6326 (Liangyou 6326) has high yield potential and wide adaptability, our results show that LY6326 is also highly sensitive to heat stress at the booting stage. Their sensitivity provides a reliable baseline for comparing the responses of hybrid varieties and underscores the need for heat-tolerant alternatives in regions prone to high-temperature events.

In contrast, TYHZ, another hybrid combination, exhibited relatively milder anther damage and a smaller reduction in seed setting rate under high temperature, indicating mild heat tolerance at booting stage, TYHZ is often characterized as a multi -panicle type variety with good tillering capacity and is also suitable for ratoon rice systems. Its better performance under heat stress suggests that TYHZ could serve as a valuable donor or candidate for breeding heat-tolerant varieties in the middle and lower reaches of the Yangtze River. whereas a previous study found TYHZ was sensitive to high temperature at flowering stage (Wang et al. 2020). It is possible that the physiological processes of pollen development, pollen germination, and pollen tube elongation in TYHZ differ in their sensitivity to high temperature, future studies should systematically compare the heat stress responses of TYHZ at the booting and flowering stages, thereby elucidating the value and limitations of its heat tolerance for breeding programs.

Under normal conditions, HHZ has a growth period of approximately 130 days for the main crop, while LY6326 requires about 139 days in certain climatic zones. Despite these differences, both short - duration (HHZ) and medium - duration (LY6326) conventional varieties showed similar heat sensitivity, whereas the hybrid TYHZ exhibited better tolerance. This indicates that the true heat tolerance is not simply determined by growth duration or phenological escape, but rather by intrinsic genetic factors related to anther wall stability, tapetum programmed cell death, and stress defense mechanisms, as supported by our ultrastructural observations. Thus, the

combination of field-scale planting data, growth duration records, and multi-scale microscopic evidence strengthens the conclusion that TYHZ is a promising heat-tolerant germplasm, while YD6, HHZ, and LY6326 require enhanced cultivation management or genetic improvement to cope with increasing high-temperature stress during the booting stage.

5.2 Response mechanisms with anatomic structures of anther under high temperature.

Male meiosis produces microspores, which then undergo further development to become pollen grains(Ma 2005). High-temperature stress causes pollen sterility and yield reduction by disrupting male meiosis, resulting in abnormal anther development, particularly the tapetum layer and microspores, which is consistent with previous studies(Hu et al. 2021; Hu et al. 2024; De Storme and Geelen 2014). The orderly degradation of tapetum cells is a key factor in maintaining normal pollen viability. In the structure of rice anthers, the tapetum is most sensitive to high temperature. Early or delayed degradation can lead to pollen sterility (Ku et al. 2003; Chaturvedi et al. 2021; Zhao et al. 2023; Hu et al. 2024). Our previous research found that the high temperature during the panicle initiation stage leads to the enlargement of the anther tapetum, which is an important reason for rice pollen sterility and subsequently reduces seed setting percentage and yield(Hu et al. 2024; Hu et al. 2021), in this study, our ultrastructural analysis revealed cultivar-specific tapetum abnormalities at stage 10 (Fig. 7). While tapetum enlargement was exclusively observed in HHZ, YD6 displayed a distinct phenotype in which tapetum contents became crowded and occupied the anther locule. Notably, LY6326 exhibited an even more severe phenotype, with the tapetum retaining only a thin cell wall and completely lacking cellular inclusions (Fig. 7). These findings demonstrate, for the first time, that tapetum hypertrophy is not a universal feature of pollen abortion across different cultivars; instead, multiple distinct tapetum degeneration patterns exist, including a previously unrecognized atrophic form in LY6326.

High-temperature stress is known to cause tapetum dysfunction, thereby impairing nutrient supply to pollen mother cells and pollen exine deposition(Ku et al. 2003; Zhao et al. 2023). In agreement with earlier work(Hu et al. 2021), our SEM analysis of pollen grains under 38 °C showed blurred exine patterns, abnormal germinal pores, and uneven Ubisch bodies (Figs. 2-6). However, we discovered that the LY6326 cultivar exhibits an unprecedented anther malformation syndrome under the same high-temperature condition. The anther locule contained only a few scattered pollen grains (Fig. 5 H); instead, most microspores remained tightly and orderly attached to the tapetum layer (Fig. 5 H, L). Moreover, the inner anther wall was completely devoid of Ubisch bodies and appeared smooth (Fig.5 I, J). Collectively, these observations define a novel developmental arrest point in LY6326: the transition from microspore release to pollen wall formation and tapetum breakdown is blocked. This finding expands the known repertoire of high-temperature-induced male sterility phenotypes and suggests a genotype-specific thermosensitive pathway.

The four varieties showed significant anther structures differences in response to high temperature. Among them, the hybrid indica rice TYHZ exhibited relatively mild anther structural damage, smaller reductions in pollen fertility and seed setting rate, and thus mild heat tolerance. In contrast, the conventional indica rice YD6, HHZ and LY6326 were more sensitive to high temperature, showing severe anther structural damage and a significant decline in seed setting rate. These differences may be related to genetic background, anther wall structural stability, antioxidant capacity, and assimilate supply efficiency among varieties.

Building on our research group's previous finding that high temperature causes tapetum swelling in two-line hybrid rice anthers(Hu et al. 2021; Hu et al. 2024), this study extended the investigation to four major varieties planted in the middle and lower reaches of the Yangtze River, including both conventional and hybrid rice, confirming that anther structural abnormality is a common response characteristic to high-temperature stress. Furthermore, by combining paraffin sectioning, SEM, and TEM, this study comprehensively revealed the multi-scale damage of high temperature to anther development from the tissue to subcellular levels, providing more systematic

morphological indicators for screening heat-tolerant varieties.

Previous studies have shown that the degradation of the tapetum is influenced by factors such as the supply of assimilates from anthers, levels of reactive oxygen species, and programmed cell death (Yi et al. 2016; Zhang et al. 2010b; Zhao et al. 2023). high temperature causes metabolic disorders and elevated reactive oxygen species levels in anthers(Yi et al. 2016; Zhang et al. 2010a; Xu et al. 2024). This study revealed divergent tapetum degeneration patterns (hypertrophy, content crowding, or atrophy) among rice cultivars under high temperature. Future work should integrate live ROS imaging, untargeted metabolomics, and in situ enzyme activity assays to determine whether each pattern is primarily driven by ROS burst, assimilate supply disruption, or altered PCD timing. Comparative analyses of cultivars with distinct phenotypes could establish direct links between ROS/metabolic signals and specific ultrastructural lesions.

In addition, this study focused only on high temperature at the booting stage, whereas in actual production, high temperature may occur at multiple stages such as panicle differentiation, flowering, and grain filling, and often co-occurs with other stresses such as drought(Kumari et al. 2024). Future research should incorporate field validation and further explore the molecular regulatory mechanisms of sugar metabolism, hormone levels, and antioxidant systems in anthers under high-temperature stress.

6. Conclusions

Through pot experiments, this study systematically analyzed the effects of high-temperature stress at the booting stage on anther structures and pollen fertility of four major indica rice varieties in the middle and lower reaches of the Yangtze River, and drew the following conclusions:

(1) High temperature significantly reduces seed setting rate and yield: Anther structural damage directly leads to decreased pollen fertility, reduced seed setting rate, and a significant decline in yield at maturity, confirming that the booting stage is a key sensitive period for high-temperature damage in rice.

(2) Hybrid indica rice TYHZ exhibits relatively mild anther structural damage under high temperature and a smaller reduction in seed setting rate, showing milder heat tolerance and serving as a candidate resource for breeding heat-tolerant varieties. Conventional indica rice YD6, HHZ, and LY6326 are relatively sensitive to high temperature and require enhanced cultivation management in areas with frequent high-temperature events.

(3) High temperature arrests anther development in LY6326 at a novel stage: after microspore release but before pollen wall formation and tapetum degeneration. Tapetum hypertrophy is not the sole cytological feature associated with heat-induced pollen abortion; atrophic tapetum (LY6326) and tapetum content crowding (YD6) represent alternative degeneration pathways. The atrophic tapetum phenotype—thin cell wall, no inclusions, no Ubisch bodies—is described for the first time in heat-stressed rice.

Declaration of competing interest

The authors declare that they have no known competing financial interests or personal relationships that could have appeared to influence the work reported in this paper.

Acknowledgements

The authors would like to thank Limin Yuan (Yangzhou University, China) for assistance with scanning electron microscopy and Wuhan Baiqiandu Biotechnology Co., Ltd. for their valuable assistance in the transmission electron microscopy (TEM) observation of anther samples.

Authors' contributions

QH and KC conceived the research, designed the experiments, analyzed the data, and wrote the manuscript. QH carried out pot experiments. WW and QL assisted in both sampling and physiological determinations in the laboratory. SP and JH gave valuable suggestions during the whole pot experiments. All authors read and approved the final manuscript.

Funding Declaration

This research was supported by the Natural Science Foundation of China

(32501827), the Natural Science Foundation of Jiangsu Province, China (BK20241855), the Lv Yang Jin Feng Talent Plan of Yangzhou City, China (YZLYJFJH2022YXBS020), the Qinglan Project of Jiangsu Province, Technology Innovation (Service) Team of Yangzhou Polytechnic University (2025XJ07) and a project funded by the Priority Academic Program Development of Jiangsu Higher Education Institutions of China (PAPD).

Availability of data and materials

All the data on the present study has been included in the tables and/or figures form in this manuscript; and the datasets used and/or analyzed in this study are available from the corresponding author on reasonable request.

Reference

Chaturvedi P, Wiese AJ, Ghatak A, Zaveska Drabkova L, Weckwerth W, Honys D (2021) Heat stress response mechanisms in pollen development. New Phytol 231 (2):571-585. doi:10.1111/nph.17380

Chen SH, Liu YH, Xiao N, Sun Y, Zhang LY, Yi XF, Xue M, Li AH, Xu ML (2026) A simplified heat-tolerance evaluation Ssystem at the pollen development stage in rice (*Oryza sativa* L.). Plants 15 (8). doi:10.3390/plants15081253

Chen XM, Xiao DP, Qi YQ, Shi ZX, Bai HZ, Lu Y, Zhang M, Pan PP, Ren DD, Yin XM, Li RJ (2025) Projected future changes in extreme climate indices affecting rice production in China using a multi-model ensemble of CMIP6 projections. Front Plant Sci 16. doi:10.3389/fpls.2025.1595367

Chen YH, Wang YL, Chen HZ, Xiang J, Zhang YK, Wang ZG, De.Feng. Z, Zhang YP (2023) Brassinosteroids Mediate Endogenous Phytohormone Metabolism to Alleviate High Temperature Injury at Panicle Initiation Stage in Rice. Rice Sci 30 (1):70-86. doi:10.1016/j.rsci.2022.05.005

Das S, Krishnan P, Nayak M, Ramakrishnan B (2014) High temperature stress effects on pollens of rice (*Oryza sativa* L.) genotypes. Environ Exp Bot 101 (1):36-46.

doi:10.1016/j.envexpbot.2014.01.004

De Storme N, Geelen D (2014) The impact of environmental stress on male reproductive development in plants: biological processes and molecular mechanisms. Plant Cell Environ 37 (1):1-18. doi:10.1111/pce.12142

Guo H, Tao W, Gao HY, Chen L, Zhong XY, Tang MY, Gao GQ, Liang TF, Zhang XL (2024) Physiological traits, gene expression responses, and proteomics of rice varieties varying in heat stress tolerance at the flowering stage. Front Plant Sci 15. doi:10.3389/fpls.2024.1489331

Hao LS, Ma N, He LY (2022) Circulation anomalies characteritics of the abnormal drought and high temperature event in the middle and lower reaches of the Yangtze River in summer of 2022. Journal of Arid Meteorology 40 (5):721-732. doi:10.11755/j.issn.1006-7639（2022）-05-0721

Hu QQ, Chen C, Wang KP, Zhang J, Huo ZY (2025) Advances in evaluation of heat-tolerant rice varieties at the reproductive stage and their resistance mechanisms. Jiangsu Agricultural Sciences 53 (23):1-10

Hu QQ, Cui KH, Wang WC, Lu QF, Huang JL, Peng SB (2021) Abnormal anther development leads to lower spikelet fertility in rice (*Oryza Sativa* L.) under high temperature during the panicle

initiation stage. BMC Plant Biology 21:428. doi:https://doi.org/10.1186/s12870-021-03209-w

Hu QQ, Yan N, Cui KH, Li GH, Wang WC, Huang JL, Peng SB (2024) Increased panicle nitrogen application improves rice yield by alleviating high-temperature damage during panicle initiation to anther development. Physiolo Plantarum 176 (2):e14270. doi:10.1111/ppl.14230

Jiang MY, Huo ZG, Zhang L, Zhang FY, Li MX, Mi QC, Kong R (2024) Dynamic evaluation and risk projection of heat exposure based on disaster events for single-season rice along the middle and lower reaches of the Yangtze River, China. Agronomy 14 (8). doi:10.3390/agronomy14081737

Khan Z, Jan R, Asif S, Maharani HA, Farooq M, Kim K-M (2026) Advancing Rice Resilience to Heat Stress: Insights from CRISPR/Cas9 Genome Editing. Rice Sci 33 (3):340-350. doi:10.1016/j.rsci.2026.02.003

Ku SJ, Yoon H, Suh HS, Chung YY (2003) Male-sterility of thermosensitive genic male-sterile rice is associated with premature programmed cell death of the tapetum. Planta 217 (4):559-565. doi:http://doi.org/10.1007/s00425-003-1030-7

Kumari S, Basu S, Kumar G (2024) A systematic review on the implications of concurrent heat and drought stress in modulating

floral development in plants. Plant Sci 349. doi:10.1016/j.plantsci.2024.112248

Ma H (2005) Molecular Genetic Analyses of Microsporogenesis and Microgametogenesis in Flowering Plants. Annual Review of Plant Biology 56 (1):393-434. doi:10.1146/annurev.arplant.55.031903.141717

Peng SB, Huang JL, Sheehy JE, Laza RC, Visperas RM, Zhong XH, Centeno GS, Khush GS, Cassman KG (2004) Rice yields decline with higher night temperature from global warming. Proc Natl Acad Sci USA 101 (27):9971–9975

Su Q, Rohila JS, Ranganathan S, Karthikeyan R (2023) Rice yield and quality in response to daytime and nighttime temperature increase – A meta-analysis perspective. Science of The Total Environment 898. doi:10.1016/j.scitotenv.2023.165256

Sun T, Miao.Tian.Hui., Hu JN, Zhou H, Yang. , Li ML, Zhang JY, Pan YY, Bi R, Ye SH, Wei ML, Wua ZY, Li GQ, Yang WG, Fang PP, Cao J, Zhang WY (2025) Quantitative assessment of heat tolerance in new rice varieties through field survey during natural extreme heat events. Eur J Agron:127749. doi:10.1016/j.eja.2025.127749

Visakh RL, Anand S, Arya SN, Sasmita B, Jha UC, Sah RP, Beena R (2024) Rice Heat Tolerance Breeding: A Comprehensive

Review and Forward Gaze. Rice Sci 31 (4):375-400. doi:10.1016/j.rsci.2024.02.004

Wang CH, Mu QL, Wang S, Tian XH (2020) Screening of high temperature tolerant rice（*Oryza Sativa* L.）varieties from current commercial varieties and materials. Hubei Agricultural Sciences 59 (20):25-28. doi:10.14088/j.cnki.issn0439-8114.2020.20.005

Wang SM, Zhang DW, Yang QJ, Wang WL, Zhu QS (2007) Research on high yield and high-temperature tolerance of dominant hybrid mid-rice varieties in Anhui Province. Journal of Anhui Agricultural Sciences 35 (5):1317-1318. doi:10.13989/j.cnki.0517-6611.2007.05.030

Wu C, Cui KH, Hu QQ, Wang WC, Nie LX, Huang JL, Peng SB (2019) Enclosed stigma contributes to higher spikelet fertility for rice (*Oryza sativa* L.) subjected to heat stress. Crop J 7 (3):335-349. doi:10.1016/j.cj.2018.11.011

Xiao K, Sun Y, Wu W, Zhou XW, Zhang ZC, Lai QY, Huang C, Xiong ZH, Xin QC (2025) Quantifying the contribution of triple compound extreme events to global yield loss of major staple crops from 1982 to 2016. Journal of Integrative Agriculture 24 (10):4078-4099. doi:10.1016/j.jia.2025.04.038

Xiong DL, Ling XX, Huang JL, Peng SB (2017) Meta-analysis and dose-response analysis of high temperature effects on rice yield

and quality. Environ Exp Bot 141:1-9. doi:10.1016/j.envexpbot.2017.06.007

Xu ML, Zhang HX, Huang NS, Li AH, Dai ZY, Liu XJ (2001) Breeding and utilization of Yangdao 6: A new medium indica variety with high quality, high yield and disease resistance. China Rice (1):24-26

Xu WB, Miao YM, Kong J, Lindsey K, Zhang XL, Min L (2024) ROS signaling and its involvement in abiotic stress with emphasis on heat stress-driven anther sterility in plants. Crop and Environment 3 (2):65-74. doi:10.1016/j.crope.2023.12.002

Xu YF, Chu CC, Yao SG (2021) The impact of high-temperature stress on rice: Challenges and solutions. Crop J 9 (5):963-976. doi:10.1016/j.cj.2021.02.011

Yamamori K, Ogasawara K, Ishiguro S, Koide Y, Takamure I, Fujino K, Sato Y, Kishima Y (2021) Revision of the relationship between anther morphology and pollen sterility by cold stress at the booting stage in rice. Ann Bot 128 (5):559-575. doi:10.1093/aob/mcab091

Yi J, Moon S, Lee YS, Zhu L, Liang WQ, Zhang DB, Jung KH, An G (2016) Defective tapetum cell death 1 (DTC1) regulates ROS levels by binding to metallothionein during tapetum degeneration. Plant Physiol 170 (3):1611-1623. doi:10.1104/pp.15.01561

Zandalinas SI, Fritschi FB, Mittler R (2021) Global warming, climate change, and environmental pollution: recipe for a multifactorial stress combination disaster. Trends in Plant Science 26 (6):588-599. doi:10.1016/j.tplants.2021.02.011

Zhang DS, Liang WQ, Yin CS, Zong J, Gu FW, Zhang DB (2010a) *OsC6*, encoding a lipid transfer protein, is required for postmeiotic anther development in rice. Plant Physiol 154 (1):149-162. doi:10.1104/pp.110.158865

Zhang H, Liang WQ, Yang XJ, Luo X, Jiang N, Ma H, Zhang DB (2010b) Carbon starved anther encodes a MYB domain protein that regulates sugar partitioning required for rice pollen development. Plant Cell 22 (3):672-689. doi:10.1105/tpc.109.073668

Zhao Q, Guan X, Zhou L, Asad MA, Xu Y, Pan G, Cheng F (2023) ABA-triggered ROS burst in rice developing anthers is critical for tapetal programmed cell death induction and heat stress-induced pollen abortion. Plant Cell Environ. doi:10.1111/pce.14551

Zhou SC, Li H, Huang DQ, Lu DC, Wang ZD, Zhou DG, Li KH, Wang CR (2012) Breeding and application of Huanghuzhan ——— A new variety with 1st class rice quality of national standard. Hubei Agricultural Sciences 51 (10):1961-1964. doi:10.14088/j.cnki.issn0439-8114.2012.10.030